Magnetic Resonance Imaging, Vol. 7, pp. 591–597, 1989
Printed in the USA.

0730-725X/89 $3.00 + .00

● *Original Contribution*

COMPUTER-ASSISTED DESIGN OF SURFACE COILS USED IN MAGNETIC RESONANCE IMAGING. III. THE DESIGN AND CONSTRUCTION OF TWO LONG TWIN AXIAL ANTENNAE FOR IMAGING OF THE WHOLE HUMAN SPINE

WILLIAM S. YAMANASHI,* PATRICK D. LESTER,* AND JOHN H. LETCHER†

*Department of Diagnostic Imaging and Radiation Medicine, City of Faith Medical and Research Center, Tulsa, Oklahoma †Department of Mathematical and Computer Sciences, University of Tulsa, Tulsa, Oklahoma

Two modified folded dipole MRI surface coils were designed, constructed and tested. These antenna which are long twin axial lines use the effective distributive capacitance resulting from the distance between two longitudinal elements to provide tuning. The principal advantage of this type of antenna is the ability to image longer objects such as vertebrae, spinal cord, and longer portions of the extremities. This type of antenna shows less localized high intensity in the image due to a more evenly distributed current pickup from the sample.

The coils were designed by calculating theoretical magnetic field distribution for the twin axial coils. These were obtained by integrating the Biot–Savart equation. This gave excellent agreement with an MR image of a di-electrically uniform phantom. As antennae of this sort are nonlinear in response, giving rise to an image intensity nonuniformity, computer software for the MR image was developed to correct the image intensity profile over the experimental volume. The software significantly improved the image quality by reducing the saturated intensity of the region near the antenna, thereby revealing detailed structure of the tissue being imaged.

INTRODUCTION

Magnetic resonance (MR) imaging has been accepted in diagnostic medicine as an important complementary modality to conventional radiography, CT, ultrasound, nuclear medicine, and digital subtraction angiography. MR is used to advantage because of its superior soft tissue contrast and its flexible scan slice orientation. The use of specialized RF coils have improved both MR imaging and spectroscopy in (i) S/N ratio and (ii) spatial localization of the RF signals. The potential of the latter is further enhanced by the special space resolving RF pulse sequences used in conjunction with these coils.[1,3,6,7]

However, despite these advantages there are some significant limiting factors in the performance of region specific RF coils currently made available by several MR scanner manufacturers. Some of these problems are (1) to provide a high S/N ratio for coils designed to cover large areas as compared to those for smaller regions of interest (ROI) is difficult to develop, and (2) the RF signal nonuniformity for specialized coils is more pronounced in general as compared to head or torso coils. Most of the existing large surface coils are aimed at obtaining optimum S/N from large cross sections of the body; however, when a small portion within the large cross section (such as a small organ) is needed to be imaged in detail, they fail to produce optimum S/N for the particular details.

Consider the equation for S/N in MR:[2]

$$S/N = \phi\gamma I(I+1)C[(QVf_0T_2)/(\Delta fT_1)]^{1/2} \quad (1)$$

where

ϕ = filling factor,
γ = gyromagnetic ratio,
I = nuclear spin,
Q = quality (or gain) factor,
V = volume of the sample to be imaged,
f_0 = resonance frequency of nucleus,

RECEIVED 3/30/88; ACCEPTED 4/10/89.

T_2 = spin–spin relaxation time,
T_1 = spin–lattice relaxation time,
Δf = bandwidth of RF signal, and
C = factors related to coil geometry.

Notice that factors that can be varied by virtue of the coil design are ϕ, $\Delta V f_0$, and C. I and γ depend on the magnetic nuclei selected for imaging (^{1}H in the present case) and T_1 and T_2 depend on both the type of nucleus and the biological tissue in which nuclei are found. The principal reasons for the failure of larger surface coils to attain good S/N are (i) unfavorable ϕ factor and (ii) large distance at the deeper region from the antenna winding causing RF signal nonuniformity which can be considered as an unfavorable C factor. In order to avoid (i) and (ii), the design of the coil should require (a) well-defined ROIs with size and depth, (b) coil dimensions closely matched to the desired ROI, and (c) the iso-gauss contour of the coil should be as uniform as possible within the volume of interest (VOI) (i.e., the ROI with depth). In the present work, we implemented the above criteria (a), (b), and (c) by developing two versions of twin axial antennae, one with $\frac{1}{16}$ and the other with $\frac{1}{8}$ wavelength from the preamplifier input to the distal ends at the antennae. The precise dimensions were calculated by the techniques defined elsewhere.[4]

THE MATERIAL AND METHODS FOR THE ANTENNA DESIGN[9–11]

The design criteria were specified as follows:

1. The $\frac{1}{8}$ wavelength antenna was to cover ROIs of the spinal cord from the upper cervical spine to the sacrum or the lower extension of the leg. The $\frac{1}{16}$ wavelength antenna was to be able to image any 44-cm length segment of the spine, knee, or foot.
2. The rectangular portion of the $\frac{1}{8}$ wavelength antenna at 21.335 MHz was set at $\frac{1}{16}$ wavelength or 78 cm, and the length between the antenna and the receiving preamplifier input was also set to $\frac{1}{16}$ wavelength, totalling 169 cm ($\frac{1}{8}$ wavelength). The dimensions for the $\frac{1}{16}$ wavelength antenna were set to $\frac{1}{2}$ of all dimensions above. The width of the $\frac{1}{8}$ wavelength coil is 12.5 cm and the width of the $\frac{1}{16}$ wavelength coil is 10.2 cm. No adjustable capacitor was used for the $\frac{1}{16}$ wavelength antenna whereas a 170 pF maximum adjustable nonferromagnetic capacitor was used in a parallel configuration with the $\frac{1}{8}$ wavelength antenna.
3. The calculation of the magnetic field intensity at a set of points was performed by the integration of the Biot–Savart equation for all components which make up the antenna. These equations were used in a generalized technique outlined elsewhere[4] to determine the coil shape and design parameters.
4. The Q of the $\frac{1}{16}$ wavelength coil was measured by the resonance frequency divided by the −3 db line width using a spectrum analyzer. The unloaded Q was 137 and the Q of 125 was obtained when it was loaded with a bottle of saline.

COMPARISON OF THEORY WITH EXPERIMENT

The theoretical field distribution obtained by integrating the Biot–Savart equation was compared to that obtained with the $\frac{1}{8}$ wavelength antenna using a cylindrical, uniformly dielectric phantom of 33-cm length and 20-cm diameter. The MR image of the phantom was obtained with a Picker MR-Vista 2055 MR 0.5 T scanner with single-spin echo (Carr-Purcell) pulse sequence with TE = 26 ms, TR = 550 ms, 256 views, 2 acquisitions, field of view equal 60 or 45 cm, slice thickness equal 5 mm and with 2D-Fourier transform image reconstruction.[9] The spinal cord and vertebrae images were taken from several normal volunteers ages 22–41. The same pulse sequences as those used for the phantom study were used. The B_1 field of the twin axial antenna were oriented perpendicular to the B_0 field of the static magnet, and to the field vector of the RF transmission coil. A pair of diode decouplers was an integral part of the receiving preamplifier.

THE COMPUTER CORRECTION OF THE IMAGE FOR ANTENNA NONLINEARITY[5]

The Picker International MR-Vista 2055 MR images are spin density functions that are calculated and stored as an array of 16-bit integer values of intensity, one for each viewable picture element (pixel). This image covers roughly a circular area and is stored on the usual archive tapes as a serpentine linear array which starts at the top of the image, and for each line, from left to right, the image values are converted to a linear string concatenated to the previous line, two bytes per pixel. Those values describe an image of very great dynamic range (at least 1 in 2^{14} or 1 in 16384). This cannot be displayed with full dynamic range on the viewing device of the imager. The displayed intensity normally has a grey scale of 1 in 256. Therefore, the intensity of the displayed image, $I(\hat{r})$, is a mapping of the calculated pixel values, $\rho(r)$, such that

$$I(\hat{r}) = I \min \qquad (2)$$

when $\rho(r)$ is less than some lower threshold ρ min, and

$$I(r) = I \max \tag{3}$$

when $\rho(r)$ is greater than another threshold ρ max, and

$$I(r) - \frac{(I \max - I \min)(\rho(\hat{r}) - \rho \min)}{\rho \max - \rho \min} ,$$

$$0 \text{ otherwise} . \tag{4}$$

If the presentation is adjusted for acceptable density and contrast at the mean density ρ mean = (ρ max − ρ min)/2, then beyond each shoulder the image is too dark or too light and visual information is hidden since all spin density values are displayed at the same intensity. With antennae of uniform response over the VOI, this works well. However, when an antenna has a sensitivity in one part of the VOI different from another part, inevitably part of the image will appear to be too dark or too light. If the calculated magnetic field for the coil $H(\hat{r})$ is a direct measure of the antenna sensitivity, it should be possible to apply a filter function to correct the calculated ρ values to produce $\rho_c(\hat{r})$. Thus, for a suitably chosen fixed point $\hat{r}_0$ (usually at the center of the VOI), we have:

$$\rho(\hat{r}) = \rho(\hat{r})\,[H(\hat{r}_0)/H(\hat{r})] . \tag{5}$$

This procedure has been applied by:

1. Obtaining an image in the normal manner. A typical result is shown in Fig. (1A). The surface coil is placed on the back shown by the vertical white line in Fig. 1(B). Please noted that the area posterior to the spinal column is burned out (too light) and the area anterior to the spinal column is too dark, due to that fact that the sensitivity is higher close to the dipole antenna.
2. An archive tape was written using standard vendor (Picker) supplied utilities.
3. The tape was read on another computer, a Data General Eclipse 200, and the filter function expressed in Eq. (5) was applied pixel by pixel. A new tape was written in precisely the same format with the same label and descriptive information so that upon rereading, the Picker MRI would accept the tape as one that it had written.
4. The new tape was returned to the Picker and the image was restored using, again, the normal vendor supplied utilities. The imager was then viewed as if it had been produced by an antenna of uniform sensitivity. Fig. 1(B) is the corrected image corresponding to that in Fig. 1(A).

No other computer-image enhancement techniques were applied; yet, these are certainly possible.

Note the flat density profile in the region of the spinous processes (the area which is posterior to the

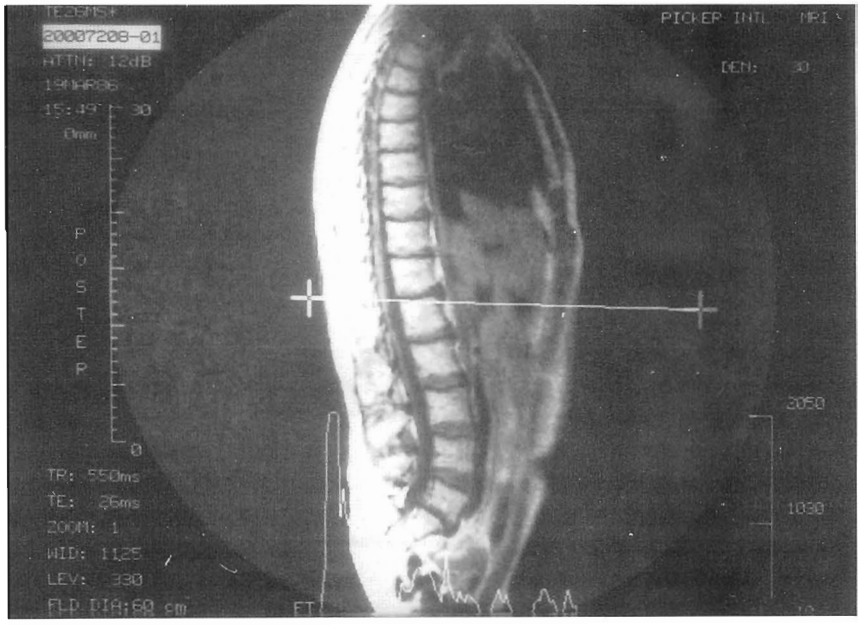

A

Fig. 1. (A) An MR image from the upper cervical spine to the sacrum obtained with the 1/8 wavelength surface coil.

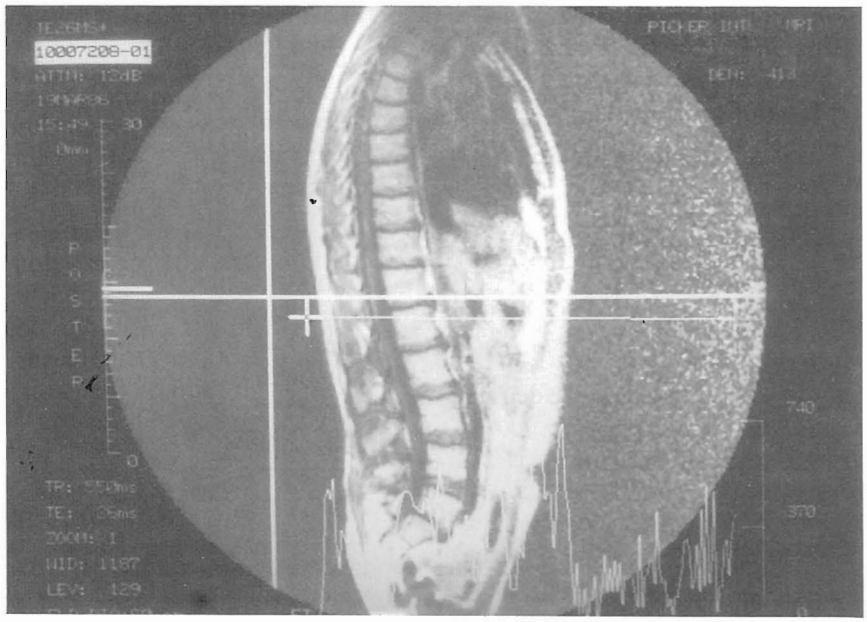

B

Fig. 1. (B) The image shown in Fig. 4(A) which has been partially corrected for surface coil antenna pattern nonlinearity.

spinal cord). Nothing can restore the information lost by this flat spot. Technicians must be warned that a repeat of the experiment must be performed after moving the patient farther from the surface coil (by inserting a 1- to 2-cm pad between the patient and the coil.

RESULTS AND DISCUSSION

A photograph of the two surface coils is shown in Fig. 2. The MR image of the phantom obtained at 0.5 T (21.335 MHz) is shown in Fig. 3 which represents the uncorrected image intensity nonuniformity. Fig. 1(A)

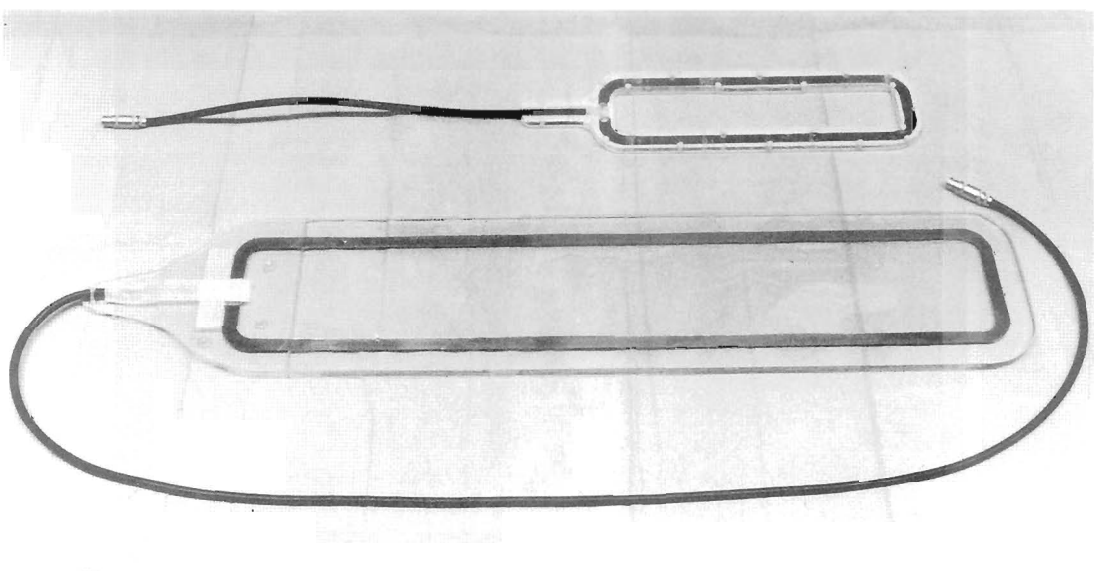

Fig. 2. A photograph of the 1/8 and 1/16 wavelength rectangular surface coils.

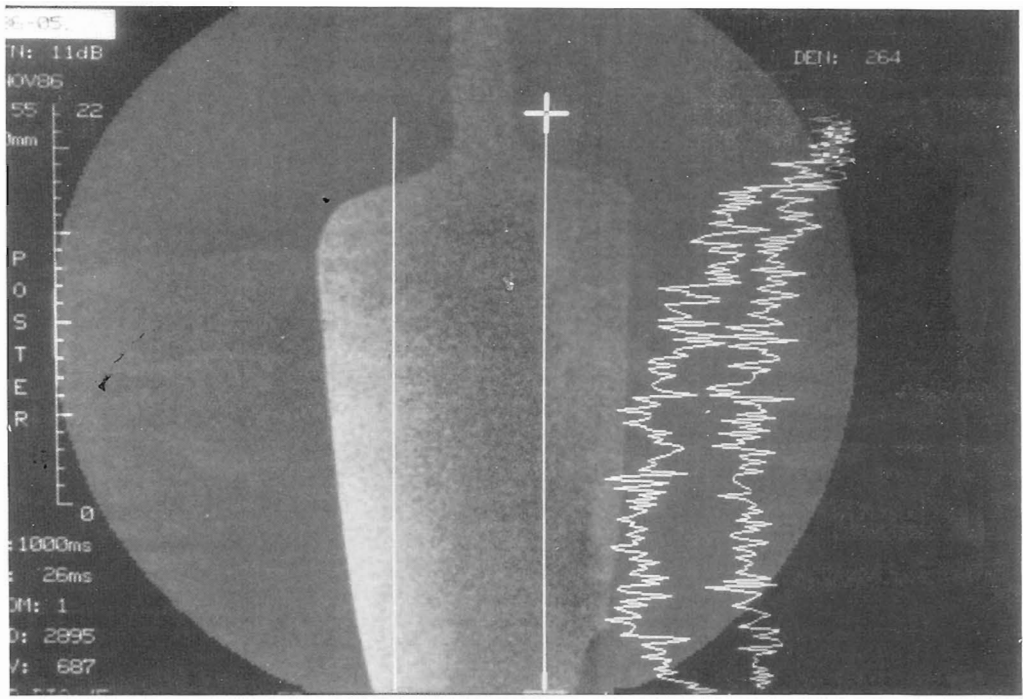

Fig. 3. The MR image of a phantom obtained at 0.5 T (21.355 mHz).

is the uncorrected MR image from the upper cervical spine to the sacrum of a 5′9″ adult volunteer, obtained with a $\frac{1}{8}$ wavelength antenna; Fig. 1(B) is the corrected MR image using the image nonuniformity compensating software. Fig. 4 is MR images of a portion of the spine, the knee and the foot obtained by the $\frac{1}{16}$ wavelength antenna.

The theoretical field distribution obtained from integrating the Biot–Savart equation and that obtained experimentally with a phantom and a $\frac{1}{8}$ wavelength antenna were in good agreement. The difference in the space distribution between the theoretical and the experimental may be due to (i) electric or E-field component of RF signal that produce time varying H-field and (ii) attenuation of RF signal due to the differences in complex dielectric permittivity and the magnetic permeability among tissues.

The comparison of the uncorrected and corrected images showed that the detailed information hidden in the saturated high intensity near the antenna may be extracted and become useful. For example, in the uncorrected sagittal image of the spine in Fig. 1(A), the details surrounding the horns of vertebral column is obliterated due to the saturated intensity. However, in the corrected image of Fig. 1(B) the contrast of the detail becomes apparent and anatomical information may be extracted.

In conclusion, twin axial antenna as a receiving probe is a simple and effective means to image the spine, vertebrae and extremities when a quick scan of the entire region is required. Further, the use of image nonuniformity compensating software is extremely important in extracting details of images obtained by a specialized receiving probe which has a typical high intensity saturation near the antenna and drop-off of intensity away from the antenna.

REFERENCES

1. Grist, T.M.; Jesmanowicz, A.; Fronisz, W.; Hyde, J.S. 1.5 T in vivo ^{31}P MNR spectroscopy of the human liver using a sectorial resonator. *Magn. Reson. Med.* 3:135–139; 1986.
2. Hoult, D.I.; Richards, R.E. The signal-to-noise ratio of the nuclear magnetic resonance experiment. *J. Magn. Reson.* 24:71–85; 1976.
3. Leroy-Willig, A.; Darrassee, L.; Taquin, J.; Sauzade, M. The slotted cylinder: an efficient probe for MNR imaging. *Magn. Reson. Med.* 2:20–28; 1985.
4. Letcher, J.H.; Yamanashi, W.S.; Lester, P.D. Computer assisted design of coils used in experimental zeugmatography by the use of rotational discrimination nonlinear regression analysis. 1985 Nov. 17–22; 21st Scientific Assembly and Annual Meeting, Chicago, IL: Radiological Society of North America.
5. Letcher, J.H.; Yamanashi, W.S.; Lester, P.D. Development of computer software to compensate intensity

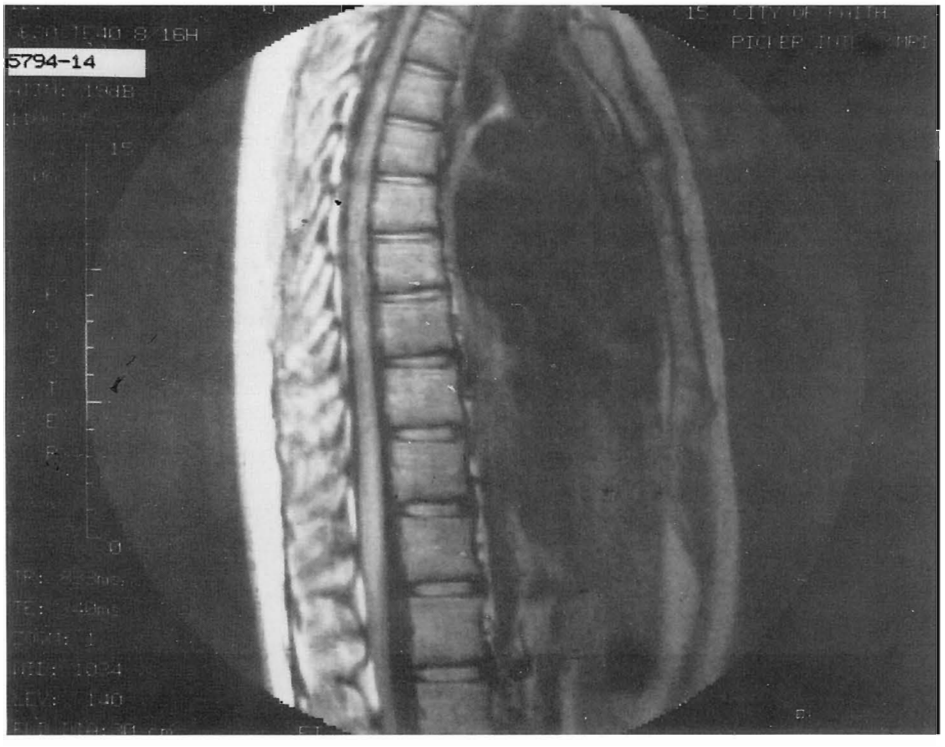

A

B

Fig. 4. (A) MR uncorrected images of a portion of the spine obtained with the 1/16 wavelength surface coil. (B) MR uncorrected images of a portion of the knee obtained with the 1/16 wavelength surface coil. (*Figure continued on facing page.*)

C

Fig. 4 continued. (C) MR uncorrected images of a portion of the foot obtained with the 1/16 wavelength surface coil.

nonuniformity in MR images obtained with surface coils. 1986 Nov. 20–Dec. 5; 72nd Scientific Assembly and Annual Meeting, Chicago, IL: Radiologic Society of North America, abstr. p. 27.

6. Sergiadis, G. Performance evaluation of whole body MNR scanner antenna system. *Magn. Reson. Med.* 2(4): 238–335; 1985.
7. Styles, P.; Scott, C.A.; Radda, G. A method for locating high resolution MNR spectra from human subjects. *Magn. Reson. Med.* 2(4):402–409; 1985.
8. Yamanashi, W.S.; Hartman, R.D.; Sy, A.M.; Crandall, C.R.; Lester, R.D. Magnetic resonance imaging of small anatomic regions, joints and vasculatures at 0.25 T using small coils of various sizes and geometries. 1985 March 22–26; 3rd Annual Meeting, San Diego, CA: Society of Magnetic Resonance Imaging, abstr. p. 57.
9. Yamanashi, W.S.; Letcher, J.H.; Lester, P.D. A $\frac{1}{16}$ and $\frac{1}{8}$ wavelength loop antenna for MR imaging of the whole spine and vertebrae at 0.5 T. 1986 Nov. 20–Dec. 5; 72nd Scientific Assembly and Annual Meeting, Chicago, IL: Radiologic Society of North America, abstr. p. 26.
10. Yamanashi, W.S.; Ross-Dugan, J.W.; Lester, P.D.; Thomas, G.S. Design, construction, and evaluation of multiple purpose receiving coils, an opensided saddle (OSS) coil and rectangular loop (RL) coil for MR imaging for brain stem, breast, orbit, C-, T-, and L-spine, sacrum, femur, knee, ankle, and foot. 1986 March 1–5; 4th Annual Meeting, Philadelphia, PA: Society of Magnetic Resonance Imaging.
11. Yamanashi, W.S.; Thomas, G.S.; Grazer, J.W.; Lester, P.D. Long twin axial antenna, a modified folded loop for MNR imaging of the whole spine and vertebrae. 1986 Aug. 17–22; 5th Annual Meeting, Montreal, Quebec, Canada: Society of Magnetic Resonance in Medicine, abstr. p. 221.